Preparation and first applications of a digital SiPM

von

Robert Joppe

Bachelorarbeit in Physik

vorgelegt der
Fakultät für Mathematik, Informatik und Naturwissenschaften
der
Rheinisch-Westfälischen Technischen Hochschule Aachen

Januar 2017

angefertigt am

III. Physikalischen Institut A

Erstgutachter und Betreuer

Jun. Prof. Dr. Thomas Bretz
III. Physikalisches Institut A
RWTH Aachen University

Zweitgutachter

Prof. Dr. Thomas Hebbeker
III. Physikalisches Institut A
RWTH Aachen University

Contents

1 Introduction **1**

2 SiPM **3**

2.1 Silicon photomultiplier 3

2.1.1 Analog SiPM 3

2.1.2 Digital SiPM 5

2.2 Readout board 6

2.2.1 Digital SiPM 6

2.2.2 Hardware 7

2.2.3 Readout software 8

3 Preparations **11**

3.1 Chip surface protection 11

3.2 Bonding wire protection 14

4 First light **17**

4.1 Setup 17

4.2 Measurement 17

4.3 Analysis 18

5 After preparations **21**

5.1 Setup 21

5.2 Measurement 22

5.3 Analysis 22

6 Scintillator - setup **27**

6.1 Setup 27

6.2 Measurement 29

6.3 Analysis 30

7 Summary and Outlook **35**

References **37**

Acknowledgements **39**

1. Introduction

The use of semiconductor-based photo sensors has increased in the last years. Especially in particle physics an efficient light detection is important. There are a lot of experiments using analog silicon photomultipliers (SiPM). Just to name a few: FACT[1] on La Palma, the FAMOUS[2] telescope developed in Aachen and different types of devices for medical imaging like the PET[3].

This thesis focuses on a new type of semiconducting light detection devices, which is called digital SiPM. This device was designed by the University of Heidelberg and built by the Fraunhofer Institute IMS in Duisburg. The potential of a digital SiPM are high, because it makes two dimensional light measurements possible.

The first chapter gives an introduction to the theory behind SiPMs and presents the digital SiPM with its hardware. After this, chapter 2 focuses on the hardware of the chip and how it can be protected against mechanical deformation. The third chapter describes first measurements made with the SiPM and will lead over to chapter 4 where the first measurements with an optical fiber will be discussed. The last chapter will present a setup with scintillator bars and a measurement of muons.

[1] First G-APD Cherenkov Telescope

[2] First Auger Multi-pixel-photon counter camera for the Observation of Ultra-high-energy air Showers

[3] Positron Emission Tomography

2. SiPM

This chapter gives a short introduction to the idea and structure of silicon photomultipliers (SiPMs). The setup of the experiment used for this thesis will also be discussed.

2.1 Silicon photomultiplier

In modern physics, an efficient light detection is very important. There are different methods to detect photons. One example is a photomultiplier tube (PMT), where photons eject electrons out of a photocathode. These electrons are accelerated and multiplied by a system of dynodes which are operating with a voltage in the order of 1 kV. In total the electric pulse is multiplied by a factor of 10^6 up to 10^8 and can be measured for example by a counter [1]. The use of PMTs is very popular in many different experiments in physics. One of these experiments is the Pierre Auger Observatory in Argentina where air-showers, created by cosmic ultra-high energy particles, are studied. The detector consists mainly of two different detectors based on PMTs. The surface detector (SD) is composed of large water tanks with three PMTs which detect Cherenkov light. The other detector is composed of 27 fluorescence telescopes (FD) with a camera consisting of 440 PMTs each. These detect the light created by excited nitrogen in the atmosphere during the air-showers.
However, there are some disadvantages of these tubes. For example, the costs of one tube are large and they are very fragile. Furthermore, the operation voltage of some kV is sometimes problematic, when closed to the high voltage wires electronics are located, and they do not work with magnetic fields. The investigation in new technologies has developed a semiconducting device for photon detection named silicon photomultiplier (SiPM) around the 2000s. These have a lot of advantages in comparison to photomultiplier tubes. The use of SiPMs in various parts of physics has increased. These SiPMs are composed of many Geiger-mode avalanche photodiodes (G-APD).

2.1.1 Analog SiPM

The avalanche photodiodes nowadays are silicon cells with a footprint size of $10 \times 10\,\mu\text{m}^2$ to $100 \times 100\,\mu\text{m}^2$ and a thickness of 0.2 mm to 0.4 mm. The basic schema of the silicon device is shown in fig. 2.1a .
The layer on top of the cell is strongly enriched with positive charge carriers (p++), also known as the acceptor. Below this there is a normally enriched layer of positive charge carriers (p+). The two positive layers are placed in a trough made of a layer

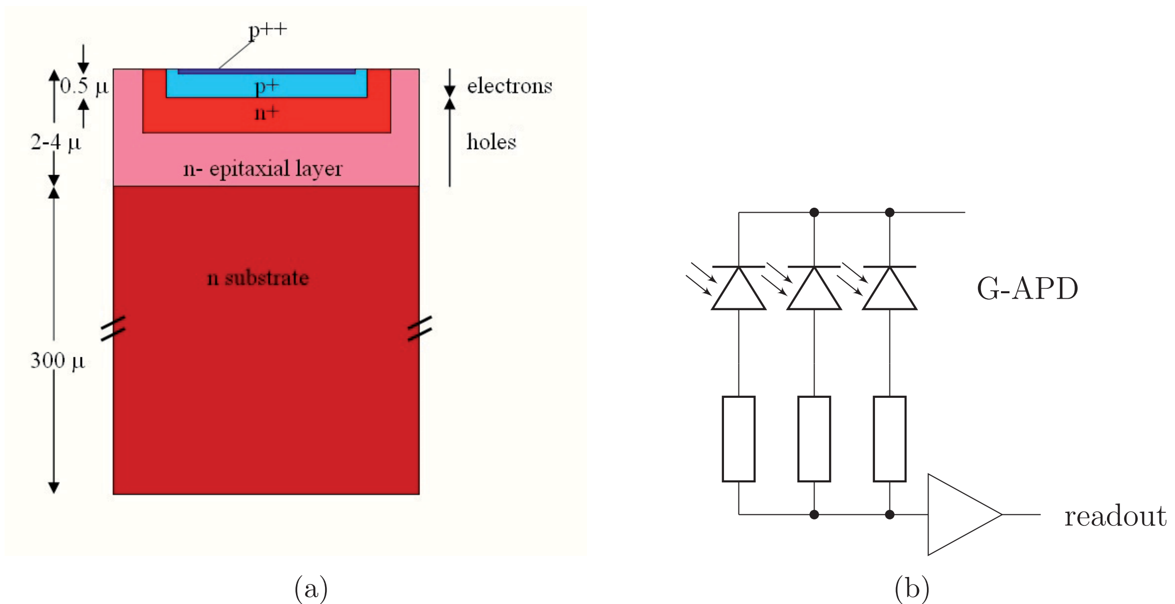

(a) (b)

Figure 2.1: a) Schematic of an avalanche photodiode. The blue marked areas are acceptors and the red are donators of the semiconducting component. Taken from [2]. b) Example circuit diagram of an analog SiPM. The APDs are connected in parallel and, through the readout parallel. The reulting signal is the sum of all cells. Referring to [3].

enriched with positive charge carriers (n-), also known as a donator. For operations in the Geiger-mode, there is a voltage applied between the first acceptor (p++) and the donator (n-) about $30\,\mathrm{V} - 70\,\mathrm{V}$. This setup creates an area without free charge carriers, but a high electric field.
When a photon hits the first layer of a cell, it emits an electron which is accelerated by the field and causes an avalanche in the donator layer. This can be measured as a decreasing of the applied voltage. In an analog SiPM many of these Geiger-mode avalanche photodiodes are connected in parallel as shown in fig. 2.1b [1].

In order to get a signal for the digital accumulation, the readout signal must be amplified. Afterwards, the signal is separated in two analysing channels. The first checks, by using a discriminator, whether the signal has the attributes to be a pulse from the chip and is not noise. Then, the signal is integrated and the time information is produced by a TDC (time to digital converter). The second channel analyses the shape of the signal and gets information about the energy of the pulse.
The advantages in relation to photomultiplier tubes are huge. The output signal is proportional to the number of fired cells. Furthermore, you get information on how many photons have been detected and the photon detection efficiency (PDE) is very similar to PMTs, depending on the wavelength and the material used. Finally another, important aspect is that the prices of SiPMs are decreasing and they are not as fragile as PMTs. In particular they are not that sensitive to magnetic fields and are not damaged by high light fluxes.
The two main arguments against SiPMs are that the breakdown voltage of the cells is temperature-sensitive and that the dark noise is relatively large. However, these

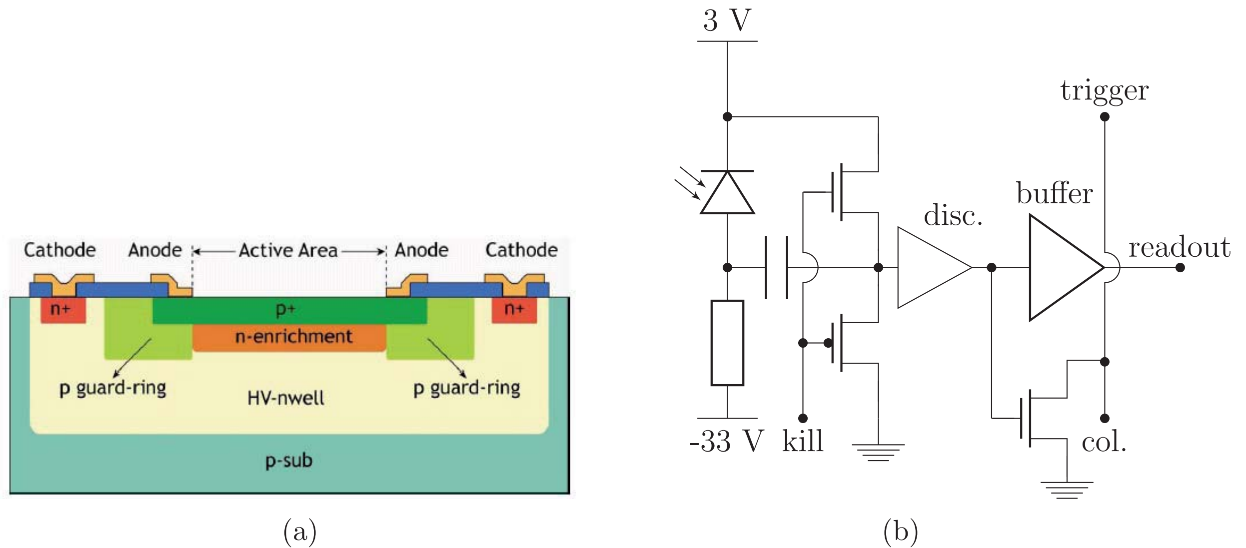

(a) (b)

Figure 2.2: a) Schematic of a Geiger-mode avalanche photodiode used in IDP 2, the digital SiPM studied in this thesis. Taken from [3]. b) Simplified circuit diagram of the basic design of one cell (disc. = discriminator, col. = column). Referring to [3].

effects are already well understood. The breakdown voltage can be corrected by measuring the temperature of the device and correcting this shift. As regards the second argument, there is a new invention where single cells can be ignored for reading out.

2.1.2 Digital SiPM

A digital SiPM is a light detection device based on the idea of an analog SiPM. The main difference is that the readout is not parallel but separate for each cell in order to get a two-dimensional image. Therefore, every G-APD is modified and has its own electronics. The cell has a „trench“ surrounding the active area which reduces the probability for optical crosstalk[1]. This effect is also supported by a guard ring around the avalanche zone as shown in fig. 2.2a. This guard ring can stop an avalanche because of the p+ abatement.

It is also possible to deactivate a single cell. On the chip this is realised by a bypass to the readout channel as in figure 2.2b. By killing cells which have a high dark count rate, the whole rate of the chip is reduced. For this the single killed cell is ignored from the whole trigger and readout network on the chip. The chip has a low afterpulsing[2] probability.
The digital SiPM has even more advantages than the analog SiPM. A comparison of the designs is shown in fig. 2.3. With the advanced design of the cells, the noise can be reduced to around $20\,\mathrm{kcps} \cdot \mathrm{mm}^{-2}$ at room temperature, when just killing cells with a high dark rate, but the main benefit is that you now have a two-dimensional image of the events.

[1]This is an effect when an electron reaches the neighbouring cell and causes a signal in it.
[2]Afterpulsing is an effect which generates phantom signals while reading the chip out.

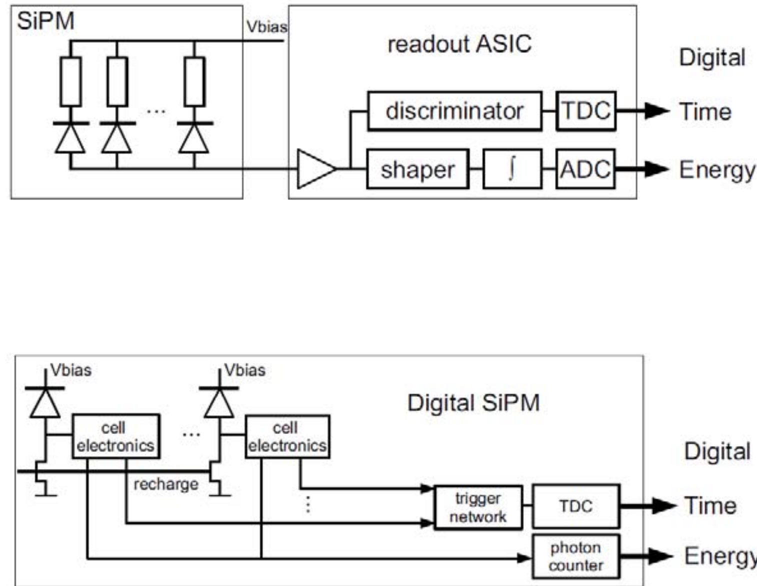

Figure 2.3: The figure shows the schematic of the two different types of SiPMs. On the top, you can see two electronic devices necassary to run the analog SiPM: the matrix of cells which consists in this circuit diagram out of a resistor and a diode and the readout ASIC that reads out the parallel signal from the cells and converts it with some logic components in a digital signal. The digital SiPM has electronics at each single cell. By reading out this chip, you get a digital signal and you just need a data acquisition and the power supply. Taken from [4].

2.2 Readout board

In this chapter, the IDP[3] 2 with its readout and support board HDROB[4] is presented. The whole chip and the board are designed by the University of Heidelberg.

2.2.1 Digital SiPM

The chip was built by the Fraunhofer Institute IMS in Duisburg using the CMOS[5] technology. This prototype has an active area of 5 x 5 mm^2 and contains 88 x 88 SPAD[6] cells. Each pixel has a size of 56.44 x 56.44 $\mu\mathrm{m}^2$ and a fill factor of 55% where photons are detected.
The design of the IDP 2 is focused on fast readout. Hence, there are eight parallel output lines which can achieve a maximum readout with 400, 000 full frames per second in theory. At the moment, the firmware version „IDP 20151201a“ allows only just a readout of 425 full frames, but a new version is in preparation [5].

[3]Interpolating Digital Photo-sensor
[4]Heidelberg Readout Board
[5]Complementary metal-oxide-semiconductor, which is a constructing method to build semiconducting devices with negative and positive enriched layers and structures for integrated circuits.
[6]Single- photon avalanche diode is a Geiger-mode operating avalanche diode.

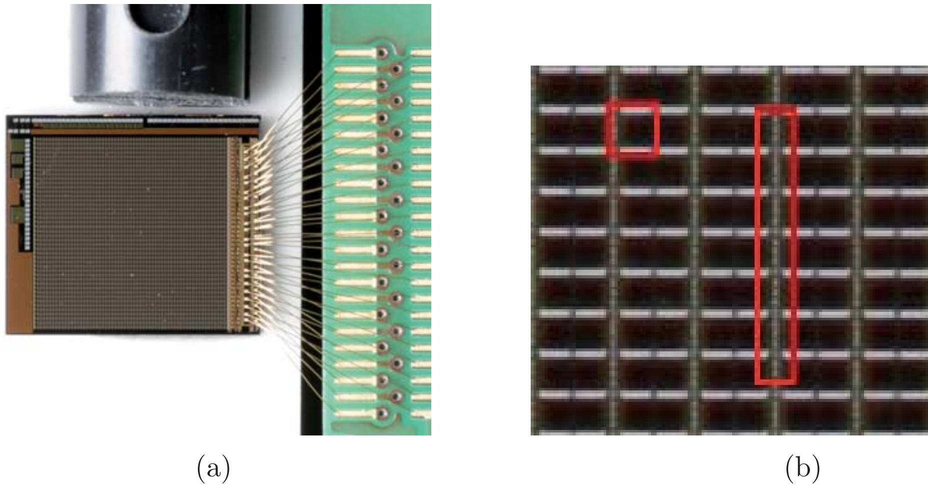

(a) (b)

Figure 2.4: a) Here is a picture of the digital SiPM shown. The chip is placed with a temperature sensor on top of a Peltier element. The SiPM is connected by bonding wires with the IDP 2 board. b) This is a section of the IDP 2 chip. The left box marks a single cell with the active area on the right and the electronics on the left side. The right box edges the electronics of many cells of two columns.

In figure 2.4a a photomicrograph of the chip can be seen. It is placed on the cold side of a Peltier device which is on top of a fin. Next to the chip is a thermometer to monitor the temperature in the direct area around the chip. The digital SiPM is connected by bonding wires to the IDP-board which is pinned on the HDROB. A picture of the cell order is shown in figure 2.4b. The cells are placed asymmetrically and share one control and one high voltage line.

In the first prototype, there was an alterable threshold at each cell, but tests have shown that this is not necessary. The chip can trigger itself. Every column has a trigger line as can be seen in figure 2.4b. These lines are connected through a multiplicity logic. This logic adds columns with a fired cell together and puts out the number of columns which have at least one fired cell. If the number is higher than a justified value, the hole data from the chip will be read out. These tiggers have, for example, the name „mult ≥ 4“. Therefore, the double data rate[7] is used to get the high readout speed. During the trigger and readout process, the cell can measure new photons after a deadtime of about 8 ns. [6]

2.2.2 Hardware

The IDP 2 is placed on the HDROB, seen in fig. 2.5. The board supports the chip and runs the device. The power is provided by a triple PSU which delivers the operation voltage of the board, the well voltage and high voltage for the chip. There is a FPGA[8] unit on the HDROB controlling the chip and supplying an interface for operating the chip. This interface can be used on a PC which is connected through a LAN port. The board has a lot of other connections, for example, to run a LED

[7] On every clock edge is a signal transmitted.
[8] Field Programmable Gate Array

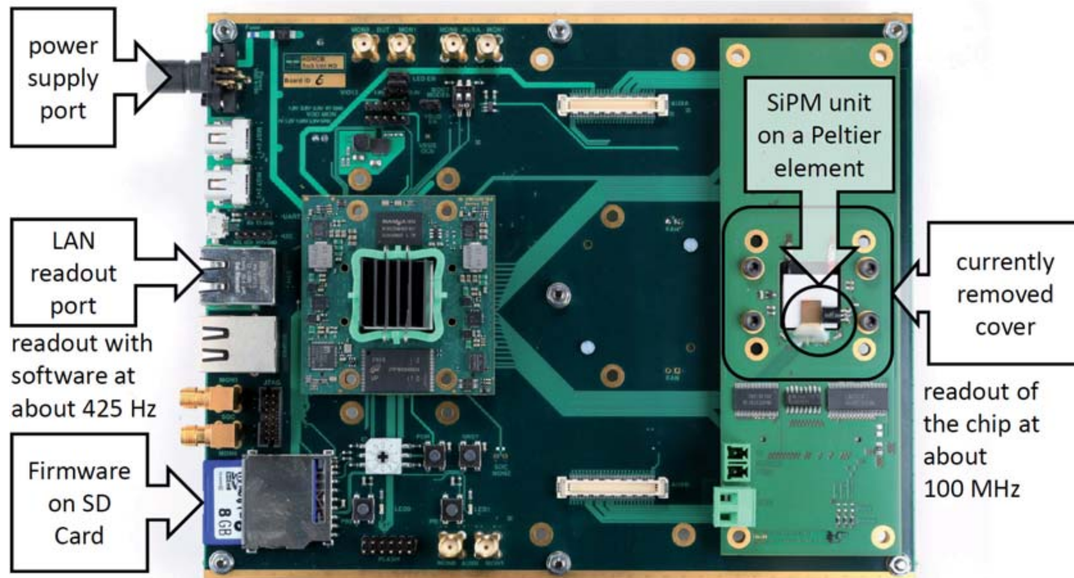

Figure 2.5: This is the Heidelberg Readout Board with the IDP 2 board on it.

or to view the output signals of the chip, but these are not used in this thesis. On the bottom side, there is a fan to cool a fin beneath the Peltier element. It is also possible to extend the board with a control unit for the Peltier element. This setup guarantees that the chip is able to operate at a stable temperature below 30 °C. In this bachelor thesis the Peltier element was not used because the temperature did not exceed 35 °C in the operation mode.

2.2.3 Readout software

The interface of the readout software is shown in a screenshot in figure 2.6. The program is written in C++ and forms a GUI. After connecting the computer to the HDROB, the temperature values are updated every second.

To control the chip, there are different options for operating. On the left side on top there is a matchbox with different trigger types. The random trigger can be activated by entering in a number in the small box next to the button and clicking this button. Then the software will collect many frames and add them to the histogram. The „Inject“ and „Pulser“ buttons start the readout with a special setup to check the time resolution of the chip. Behind the „digital Mux 0“ - „digital Mux 2“ are variable self-trigger options. They can be set in the panel called „IDP Settings“. Among others, there are multiplicity triggers with different minimum values chosen. If one of the triggers is enabled, the GUI begins to collect events from the FPGA. If the HV is high enough, the hit rates will show the event rate in frames per second [7]. In the first panel, the last collected event is shown. The second panel, called „Accumulated“, shows a two-dimensional plot where all collected events are summed up. To increase the contrast in the histogram, it is possible to display the whole histogram in a square root scale. Here, it is also possible to save the image as an ASCII file. With

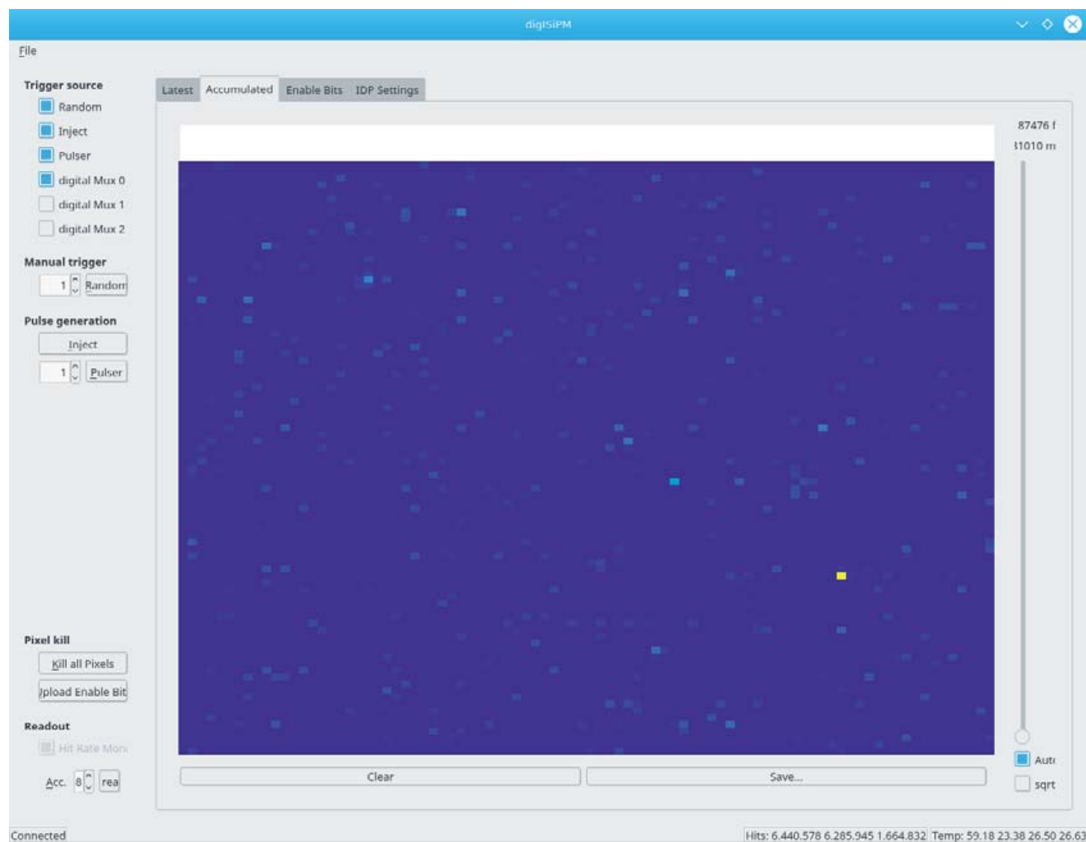

Figure 2.6: Here is the interface of the readout software shown. The first trigger is activated and takes data from a measurement in darkness.

the clear button the histogram will be reset to zero. By clicking on one pixel in the plot it is possible to kill a single pixel. With the same procedure, the pixel can be reactivated. By clicking on „Kill all Pixels“ all pixels are turned off. After this it is possible to upload the enable pixel by clicking the button below. Then the chosen pixel is deactivated.

In the panel „Enable Bits“, it is possible to kill all pixels on command and enable them. The last panel is for configurations and the choice of the self-trigger type.

For later experiments, I modified the software lightly. After this, the GUI saves single frames in an ASCII file, if the frame's hit value[9] is higher than a chosen value. Nevertheless, the program saves the hit value of every collected frame.

[9]This is the sum of all fired cells in one frame.

3. Preparations

To use the digital SiPM for further experiments the setup on the IDP 2 board is not sufficiently protected. For example, the bonding wires[1] which connect the chip with the board are very fragile. Also, there is no information about the coating[2] on the chip.

3.1 Chip surface protection

The main thought behind the protection of the surface is to allow the placing of different types of optical components on top without damaging the chip. Due to of the advanced features of the digital SiPM it is possible to investigate the structure of the light output of several optical components, especially optical components which are used in different experiments using analog SiPMs. Special emphasis is put on the analysis of the light output of wavelength shifting fibers (WLS). To analyse them, the fiber must be placed as closely as possible on the chip without touching the sheer surface.

Since this is quite difficult, I decided to build a protection for the surface. My first idea was to place a glass plate on the chip. The chip would then be secured under the plate and the light transmission would be okay for the aspired experiments. However, the problem with this idea are the bonding wires of the SiPM.

To verify the consequences if the chip is not protected I acquire a CCD chip for destructive tests. Therefore, I used an old chip of a camcorder with smaller bonding wires than those of the SiPM, shown in figure 3.1. The CCD chip is about $3 \times 5\,\mathrm{mm}^2$ and was placed in a small box of plastic, covered with a 1.3 mm thin glass plate. The scratches on the top of the chip are made by touching the chip with a fragment of the glass when breaking the glass to get access for further tests. I have touched one of the bonding wires and it broke as expected. I need a new approach, so I tried another possibility

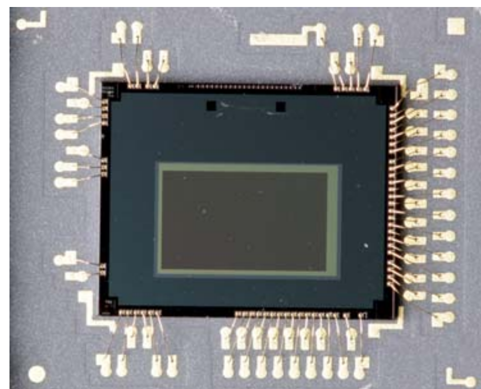

Figure 3.1: Chip for testing the possible damage while using a not protected chip in an experiment.

[1] These are very thin gold wires with a diameter around some $10\,\mu$m.

[2] The coating is a thin layer above the ADP cells to protect them against dirt and humidity.

using optic gel. This does not damage the bonding wires and even improves the optical coupling of the optical components and the chip. However, this gel incorporates dust or dirt particles. Gradually the gel will become less transparent. Exchanging the whole gel would also be difficult as then the chip could be damaged. Another problem is that the gel touches the gold wires and perhaps causes an electrical short. To sum up the requirements for a safe surface protection, the cover of the chip has to prevent the chip against mechanic violation, must not conduct electricity and shall be cleanable. The solution is to combine the two approaches.

To realise this, the requirements of the components used are high. A glass which transmits light at a wavelength of 520 nm [3] and is scratchproof and stable against mechanical stress was necessary. The first glass which fulfilled the requirements was the Borofloat 33 produced by SCHOTT Technical Glass Solutions GmbH. The thinnest thickness is 0.7 mm and it has a transmission coefficient of 93 % at 520 nm [8]. This is thin enough to transmit most of the light, but the plate just needs to cover the surface of the chip. For thus, the glass plate shall have the size of 5 x 5 mm^2. After some research, I found a company in Aachen which has the technology to cut optical glass into small pieces. To cover not just the active area, I ordered a few pieces with the dimensions of 6 x 6 mm^2. The company called Aachener Quarz-Glas Technologie Heinrich produced the small plates as a sample for free. The quality was very good, but it was not possible to produce them without little leaps at the corners of the edges of the sides.
To get an alternative, I searched for applications which apply even thinner glasses. For microscopy, there are glasses with a thickness of around 0.13 mm used to cover objects for examination. These cover slips are made of a glass similar to the Borofloat. I procured plates with a size of 0.13 x 15 x 15 mm^3.
The difficult part now was to cut out the required plate of these thin pieces. Therefore, a lot of tries were necessary. At the final procedure, the glass is broken twice between gloved fingers. The first break must be against the preferred breaking direction[4] because the plates are square and finding the right direction is randomly. If the first breaking was successful, the piece could be broken to the final size. Other methods like holding the plate with pliers or using glass manufacturing tools were not successful as the thin glass broke immediately. The plates made by this procedure achieved not quite in the required size, but two sides came together in an angle of 90 °.
To hold the glass plate in place, I chose to use optical glue instead of gel. This also prevents the plate from damaging the bonding wires. The glue must have optimal optical characteristics, a high spectral transmittance and must be an electrical isolator. Also, the solvent must not attack the silicon. Another important point is that the glue must have a similar index of refraction in comparison to the glass to prevent total reflections. The Borofloat has an refractive index at 546.1 nm of 1.473 and the cover slip has an index about 1.525 at the same wavelength. After some research, I

[3] This is the wavelength with the highest probability of the light from the WLS fibre.

[4] These preferred directions develop while the production by cooling from the molten state to the solid state.

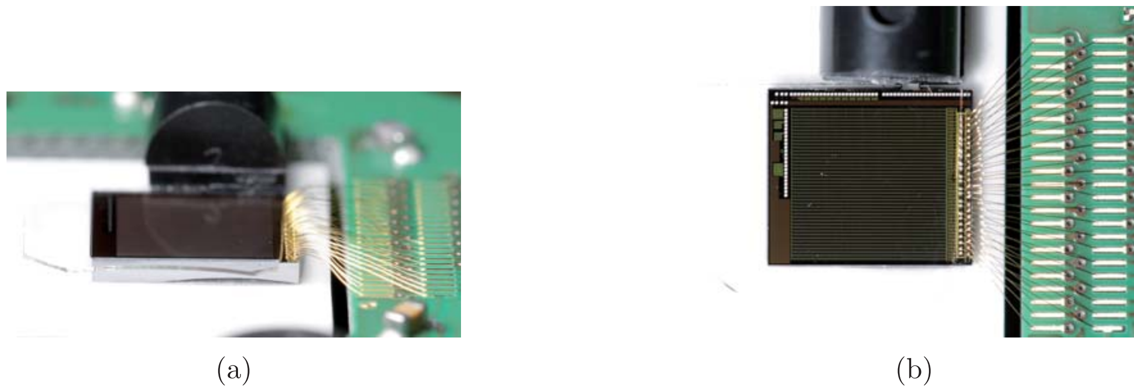

(a) (b)

Figure 3.2: Two photos of the digital SiPM after glueing the glass plate on the chip. a) SiPM with the thin glass on it. b) Chip viewed top down with the glass plate just touching the bonding wires.

found a two component glue produced by Epoxy Technology. The EPO-TEK 310M-2 has a spectral transmission of $> 98\,\%$ in the range of $380\,\text{nm} - 1660\,\text{nm}$. The index of refraction is 1.494 at 589 nm. The glue is specially designed to be used with semiconducting devices and does not harm silicon. To cure the EPO-TEK 310M-2 it must be heated up to 65 °C for at least 2 hours. Another way for curing is heating the glue up to 55 °C for 3 hours [9]. I chose the second option. The combination of the glue together with the 0.13 mm thin cover slip was the more promising way. As the glass has a higher index of refraction than the glue at the interface of the two materials, there would not be that much reflection. To get optimal results, I tested the procedure with sample glass plates and microscope slides. The benefit of this combination was that I was able to analyse the glued area bilateral if there were any air bubbles. To get the best results, I first cleaned the glass plates using an ultrasonic water cleaner. For the test, the glue must be mixed using two different components in according with the weight. Then, I made some tests to find out the right method to dip the glue. Therefore, I used a syringe with a fine cannula. After the glue was dried in a Peltier device heated oven for nearly 3 hours I could check the result. The test glueing was successful and promised that the chosen procedure would be successful.
Before glueing the cover slip onto the chip, I tried to clean the chip. For this I first blew the little dust particles away with a small bellows. In a second step, I used a statically charged brush. After charging the brush, I moved it above the chip without touching it. Unfortunately, this was not very effective. Nevertheless the particles were reduced to just a few. The best method to place the glass was to first place a drop of glue on the chip's centre. Then a side of the plate was pulled through the glue and carefully placed down in direction to the thermometer. After this, the plate could be gently slid towards the bonding wires. All these steps were executed under a binocular microscope with tweezers. The whole procedure turned out to be very successful and the result is shown in figure 3.2. The glass now covered the whole chip and just touched the bonding wires upon which the focus in the next section.

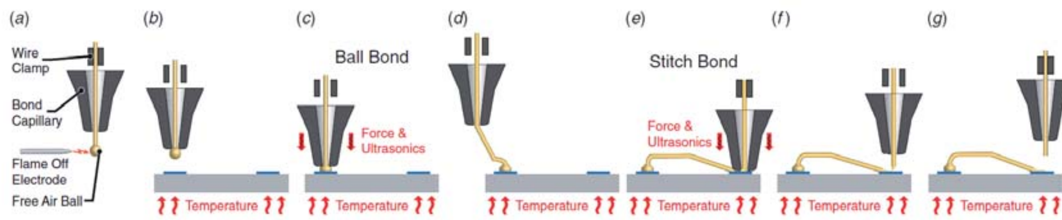

Figure 3.3: The gold wire is placed in a ceramic bond capillary and gets an electric flame off to create a free air ball at the end of the wire (a). Then, the ball is placed on top of the semiconducting device (b). With applying ultrasonics and pulling the tool on the device, the die is formed (c). After this the wire itself is created (d+e). The connection to the pad is created as before by using the force, ultrasonics and heat. The wire is torn off by closing the wire clamp and moving the bond capillary straight up (f+g). From [10].

3.2 Bonding wire protection

To connect semiconducting devices to printed circuit boards, the most commonly used method is the use of bonding wires. These wires are made out of gold which has the advantage that the electric resistance is not too high and the wires are impervious against humidity. In figure 3.3, the construction process is shown. Normal bonding wires are $20\,\mu\text{m} - 50\,\mu\text{m}$ thick. The final profile is displayed in fig. 3.4. The wires used on IDP 2 are about $30\,\mu$m thick and about 5 mm long. In normal applications bonding wires are either protected by building a case around the chip or by glueing the chip and the wires in the glob top procedure. For this, the whole setup is capsuled in a shell. The first method would not be useful because the spatial resolution suffers and the whole setup is not built for this. The second method has the problem that the chip has to be light sensitive and light would not come through the material of a glob top. However, to protect the bonding wires on the IDP 2 board, I came up with an idea based on the glob top procedure. Therefore, I intended to build a kind of dam, including the wires. This dam should protect the wires against mechanic damage. The demands were high: first I needed a material which is an electric isolator, does not attack the optical glue and is viscous to be formed without flowing into the gap between the board and Peltier element. For the glob top procedure the most common material used is based on Epoxy. This synthetic resin complies with all these demands. I chose to use a glue made by Panacol, named Vitralit 1671 [11]. This adhesive can be dried by using ultraviolet light provided by UV-LEDs. However, this glue is not transparent. So I had to take care that it does not get onto the chip's surface. To get familiar with the glue, I tested the glue on several devices. For the right placing, I used a syringe with a fine cannula. With this combination,

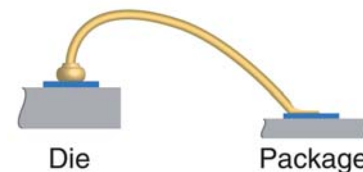

Figure 3.4: Schematic of a bonding wire used to connect a semiconducting device to a printed circuit board. Taken from [10].

I was able to form the drops of trickle. I tested the gluing on the earlier mentioned camcorder chip shown in fig. 3.1.

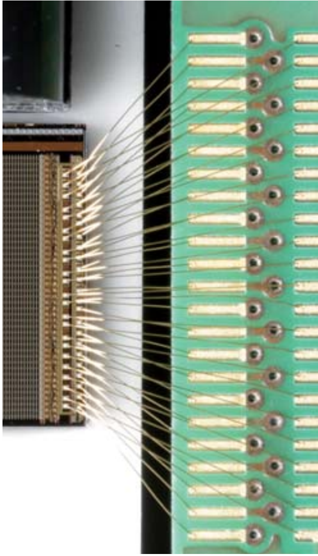

Figure 3.5: 26 bonding wires which connect the SiPM chip with the IDP 2 board.

First, I tried to just place a drop on the wires, but this was not that effective due to the surface tension of the glue. Another problem was that I had no control over the drop, whether it will drift onto the chip or onto the board. For the drying of the glue, I used three UV-LEDs for about 8 hours. After the glue had dried, I tested the stability of the Epoxy with a cannula. I just let the peak fall on to the protection and nothing happened. Then, I tried to push it into the resin, but only after a few times of pressing I was able to drill a hole in the glue. This, however, would not happen to the final protection on the SiPM. So I decided to make a second test with another way of placing the glue. Therefore I placed the trickle to the package of the wires and then pulled the glue slowly and softly in the direction of the die. This technique has the big advantage that I could minimise the amount of glue on the surface of the chip. Also, the glue now would not flow into the gap because the bonding wires would operate like steel shores in concrete. The test on the test chip went well and the glue also achieved the same stability as in the first test.

For the protection, I used about 0.4 ml of Vitralit 1671. The glue dried for about 36 hour under UV-LEDs to be sure that it has dried. The result is shown in figure 3.6. In the left picture, you can see that the trickle did not touch the active area of the chip. The small drop is optical glue from the surface protection which is visible because of the different lighting. Even this does not touch the sensitive area. In the second picture, the chip is viewed under a high angle to see the glue which forms a bridge form the side. In comparison to the chip, I could estimate the thickness of the bridge to 1 mm. This is thick enough to secure the stability of the protection.

After these modifications, I tested the functionality of the SiPM. In comparison to the tests before the preparation, there are no significant differences between the results.

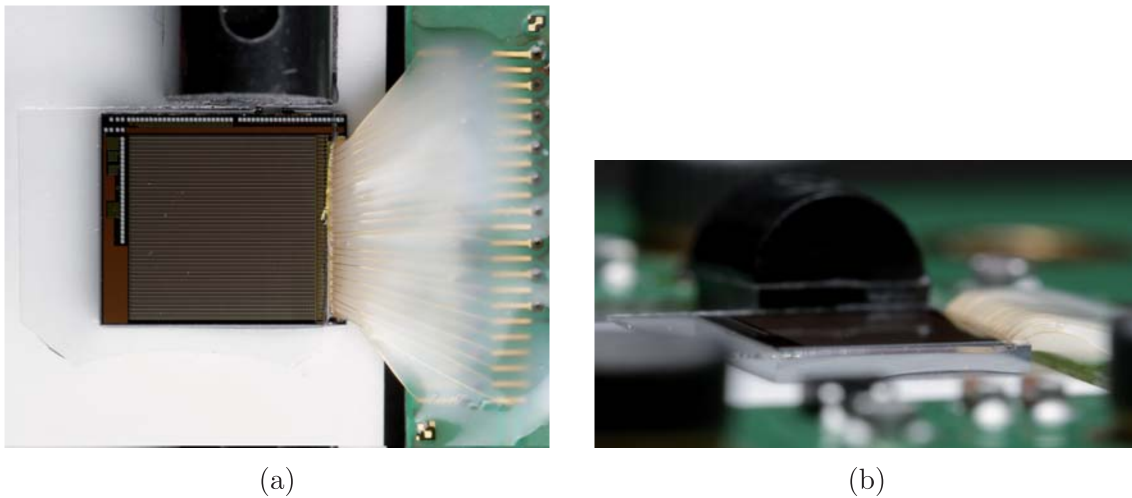

(a) (b)

Figure 3.6: Two photos of the chip with fully protection of the surface and the bonding wires. a) Full protected chip with the glass plate and the bonding wire protection. b) Chip viewed from the side to show that the glue has not flown between the Peltier element and the printed circuit board.

4. First light

The first measurements made with the digital SiPM were for characterising and finding the right parameters for operation.

4.1 Setup

For the first test, the complete HDROB setup is used. The power is supplied by a triple PSU. For the readout, a PC is used. To achieve stable temperature conditions, the setup is located in a tempered room with about 26 °C. The SiPM is covered with a 3-D printed lid shown in figure 5.2. This allows operation in the darkness. For ensuring the dimming, two measurements were made: one with a light tight layer of fabric around the whole board and another without this extra light cover. The result of these short measurements confirms that the black cover is light tight.

4.2 Measurement

The first measurement was to verify the thermal noise[1] of the chip. For this, the trigger with a threshold of one fired cell was used. The measurement is shown in figure 4.1. The noise is homogeneously distributed over the chip. Figure 4.2 shows the analysis based on the data of the measurement in fig. 4.1. Only ten percent of the cells have clearly a higher dark count rate than the others. Together these ten percent are responsible for about 77.5 % of the whole noise of the chip. However, 92 % of the cells did not fire more than 30 times.

After this, the first measurement series was for analysing at the behavior of the dark count rate at different voltages and different types of triggers. The results are shown in fig. 4.3. For these measurements, the hit rates were taken. These values can compared with the thermal noise rate of an analog SiPM. The order of magnitude for an analog SiPM is estimated on the following formula [12] :

$$f_{\text{thermal noise}} = 50\,\text{kHz} \cdot \text{mm}^{-2} \text{ at } 25\,°\text{C} \tag{4.1}$$

This formula predicts a noise rate to 1.250 MHz. This fits perfectly with the measured rate of the „mult $\geq$ 3“ trigger. The one other triggers has a higher rate as the appearance of an event with less than three fired cells is more probable. The „mult $\geq$ 4“ trigger has a smaller dark count rate because a dark count event with more than four fired cells is less probable.

[1] Thermal noise is an effect which causes a ghost signal on the chip.

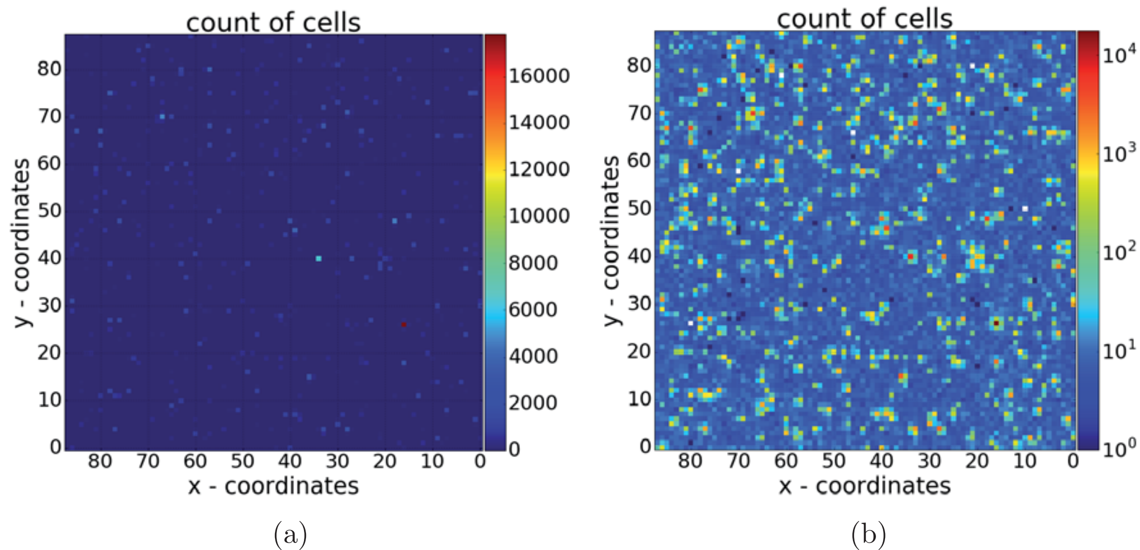

(a) (b)

Figure 4.1: The overvoltage was around 2.3 V and there were 100, 000 frames collected. The whole measurement took about 235 s. The noise is equally spread over the sensitive area. a) The color is linear to the values. The noise is spread very homogeneously over the chip. There are a few hot pixels with a higher rate. b) To get a higher contrast, the color is referred logarithmic. It is now possible to see more warm pixels, especially around the hot pixels.

An effective way to decrease the noise would be killing hot pixels. Only about 200 hot pixels are responsible for 50 % of thermal noise. These 200 pixels make 2.5 % out of the active area.

For the further measurements, I chose the trigger with the lowest dark noise, „mult ≥ 4“. To get enough PDE[2], to detect light events with less than 20 photons, I used an overvoltage[3] about 2.5 V to 3 V.

4.3 Analysis

In figure 4.1b nearly each hot pixel has warm neighbours. To analyse these, three hot pixels with neighbors are shown in figure 4.4. To be able to compare the pixels in the shown figures, they are all normed in the shown area. The pixel in figure 4.4a is the hottest one on the chip. With this pixel, I could confirm the results of more elaborated measurements [3]. These estimate that the crosstalk probability will be less than 2.6 %, on the IDP 2 chip, which is consistent with the measurement in figure 4.4a. In the other figures, pixels are shown where the results are different. The reason for this may be warm pixels which have a higher dark count rate than normal pixels. Figure 4.4c has four in vicinity of the hot pixel. These warm pixels make it difficult to analyse the crosstalk probability. In these figures, it is also possible to see the asymmetry of the cells' order. In figure 4.4c, the pixels in column

[2]Photon Detection Efficiency

[3] $U_{\text{overvoltage}} = U_{\text{operating voltage}} - U_{\text{breakdown voltage}}$; $U_{\text{breakdown voltage}} \sim 27.5\,\text{V}$

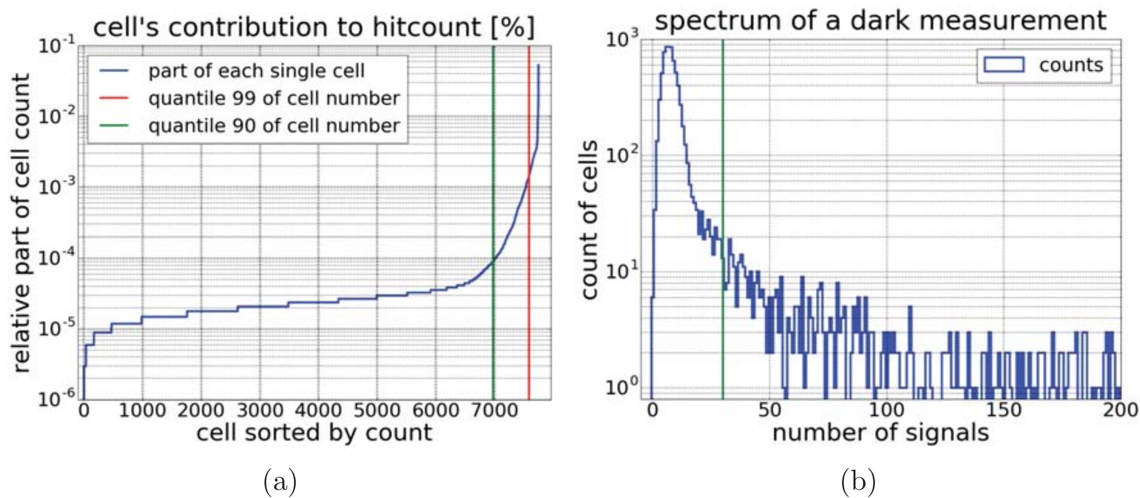

(a) (b)

Figure 4.2: a) The plot shows the relative count part of each single cell to the whole noise signal. The cells are ordered from the cell with the smallest count to the cell with the highest count. Over a quantile of 99, there are only very hot pixels which introduce a big part of the noise (about 36 %). If these were killed, the noise would be reduced obviously. The highest ten percent of cells are responsible for about 77.5 % of the summed up noise counts.
b) The histogram shows the spectrum of the number of signals. It is limited to 200 because above there are only a few hot pixels. About 92 % of the pixel did not fire more than 30 times.

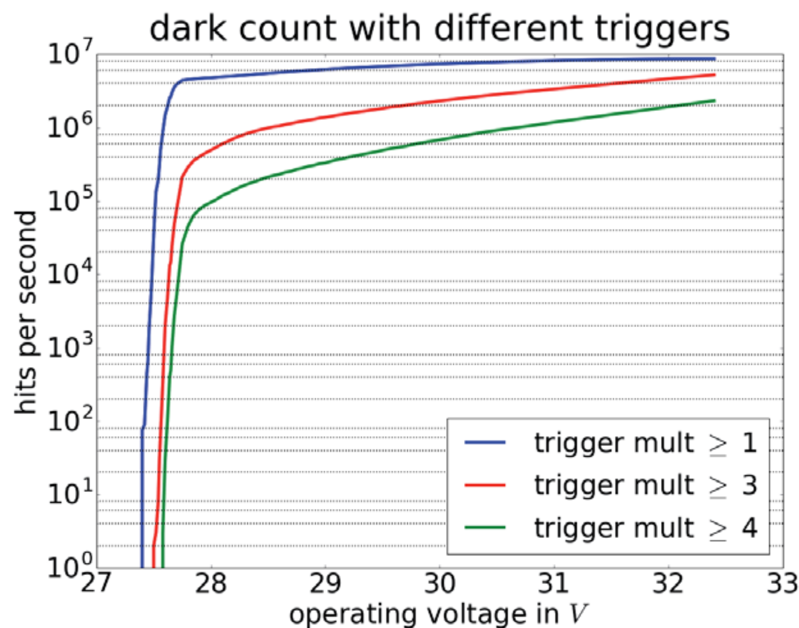

Figure 4.3: In this graph, the trend of the dark count is shown in relation to the trigger used. As expected, the trigger with the highest desired value has the minor rate. At an overvoltage of 2 V, the chip has a noise rate of 6.8 MHz, by using the trigger with the lowest multiplicity threshold. The trigger "mult $\geq$ 4" has a noise rate about 0.5 MHz.

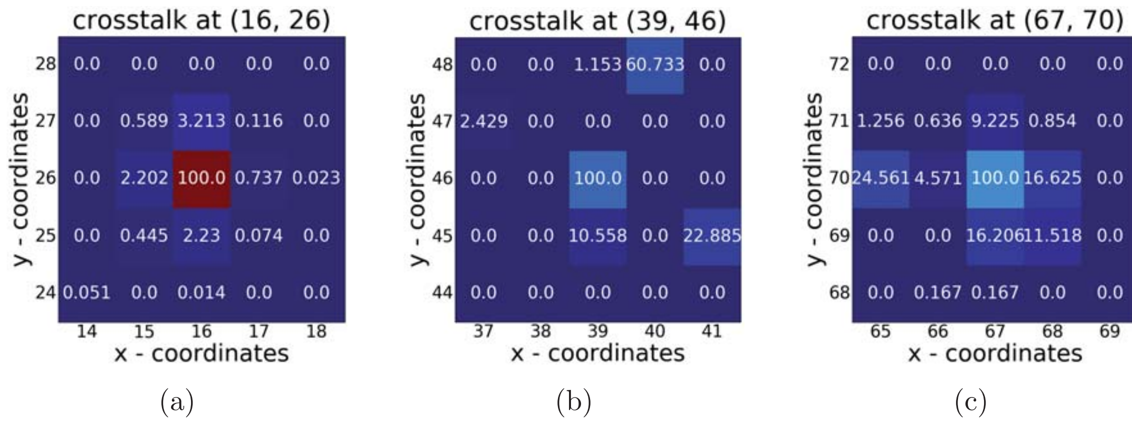

(a) (b) (c)

Figure 4.4: In the figures above, three hot pixels are shown. To be independent of the noise, the count of the surrounding pixels are averaged as the normal thermal noise and subtracted from all counts. Negative counts are set to zero. The count of every other pixel is divided by the highest count in the area to show how high the probability for crosstalk is.

67 and 68 have their active area close together. This attracts attention because the crosstalk probability in this area is similar than between 66 and 67 or 68 and 69. In figure 4.4a, this can be observed, too. The conclusion of this might be that the dark count rate of each pixel is depending on the neighbors' dark count rate in two rows where the active area is close together.

5. After preparations

After the digital SiPM has been modified, it is necessary to look whether its properties compared to before the preparations have changed.

5.1 Setup

The first measurements use the closed cover lib to allow dark measurements. In the following measurements, the setup shown in figure 5.1 and 5.2 is used. A wavelength shifting (WLS) fiber is put onto the surface of the protected chip. The end of the fiber is cut with a scalpel to be as flat as possible. Then, the end is pushed on a 150 °C hot glass pane for a very short time. This improves the transmission of light of the fiber's end as the different layers of the fiber are molten together and to improve the smoothness of the endings [13]. The cover of the whole setup with the light-tight blanket enables some photons pass to the WLS fibers. So it is possible to measure the light output of the fibers. These photons are produced by the lamps in the room. By turning these off, the whole setup is surrounded by darkness.

Figure 5.1: Here the whole setup is shown. There are 16 scintillator bars with 16 WLS fiber pairs. Each fiber pair runs parallel trough two separate bars and the endings are placed in the big "Cookie".

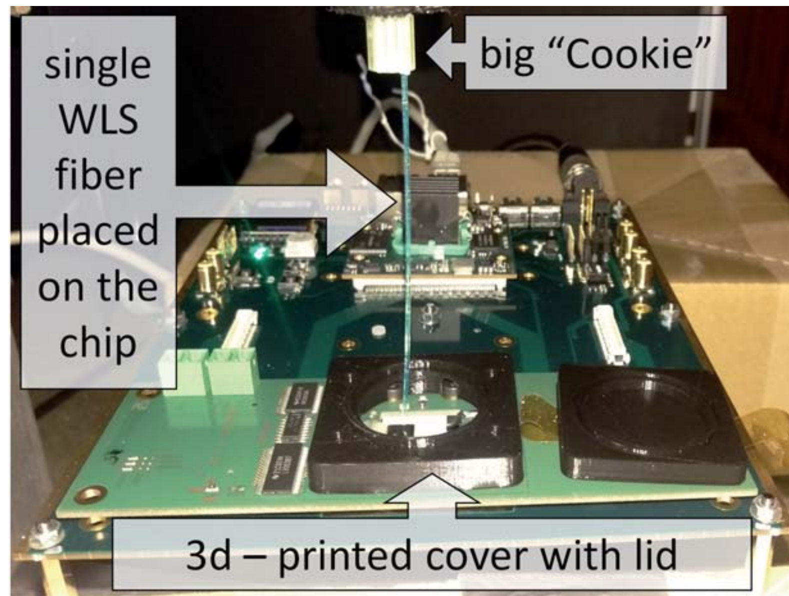

Figure 5.2: Here you can see the setup with a single WLS fiber.

5.2 Measurement

In figure 5.3, two measurements, before and after the preparation, are shown. The new binning magnifies the differences between the two pictures.

The first measurement with a WLS fiber on the protected chip is shown in fig. 5.4. For this measurement, $20,000$ frames were collected.

5.3 Analysis

For analysing the light output of the fiber, in figure 5.5 there is a „zoomed in" picture of the fiber. The plot in the upper right corner shows the raw signal in a linear scale. It is easy to identify two hot pixels and some warm ones. Since they would distort the analysis, their counts are adjusted. A script identifies these pixels automatically. The properties, whether a pixel is detected as a hot or warm one, are shown in table 5.1 and are referring to four neighbors.

These pixels are then adjusted by the mean count of the surrounding eight pixels and marked with a white "X" in the plot. In the two histograms, the counts of the picture are summed up in relation to the two orientations. The light tends to come out on the upper section of the ending, but as shown in the right histogram, this is

Properties	Hot pixel	Warm pixel
count is higher than the 3.5-fold off the global mean	yes	no
count is higher than the mean of the small neighbors times 3.5	yes	yes
more than 3 neighbors have smaller counts	yes	yes

Table 5.1: Table with the properties if a cell is identified as a hot or warm pixel.

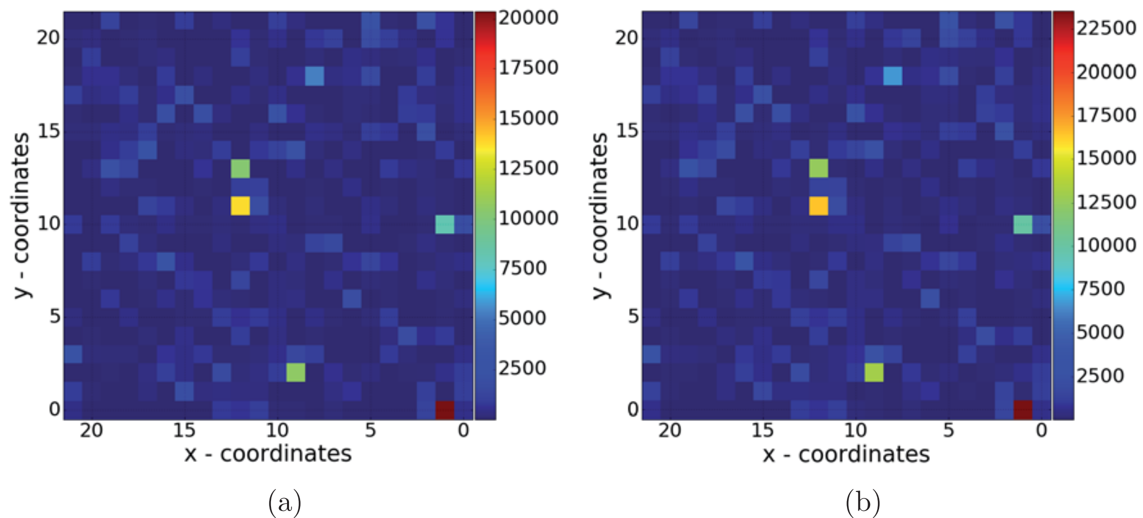

Figure 5.3: Here, two different dark measurements are displayed. The first (a) was taken before the chip has been modified and the second (b) afterwards. To be able to compare the results better, 16 pixels are rebinned to one new bin. The pictures are very similar, but the scale is a bit different. The chip now fires a little more dark noise as the temperature was a bit higher. This is not a problem since the whole dark count rate can be reduced by killing the hot pixels that are mainly responsible for the noise.

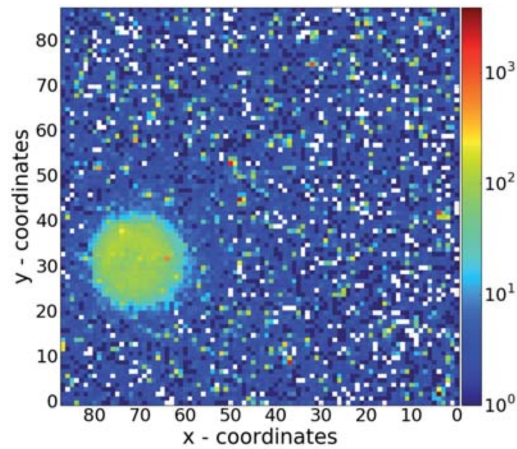

Figure 5.4: Measurement with a wavelength shifting fiber placed on top of the chip is shown here. By counting the fired cells in a row to 18 ± 1, the diameter of the fiber can be calculated as (1.00 ± 0.05) mm. According to the manufacturer, the diameter is 1 mm which is consistent with the result.

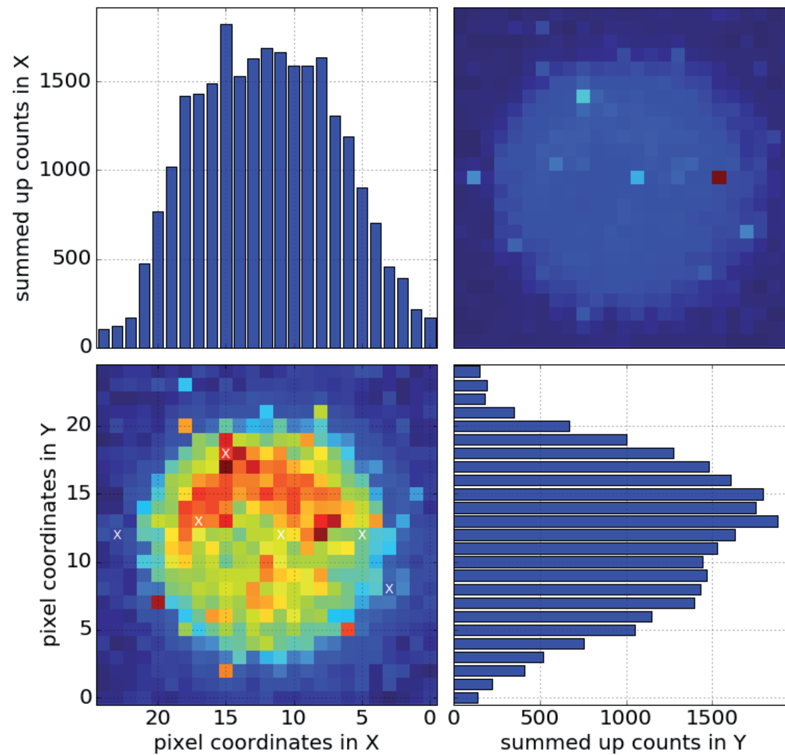

Figure 5.5: The upper right plot is the raw signal. The other plot shows the signal, which is analysed. The cells marked by white „X“ were detected as hot or warm pixels and the count is adjusted by the mean of the eight neighbors. The two histograms are the projections of the counts in one dimension.

not quite significant. The main reason for this difference is the cutting process of the fiber.

For this test setup, it was necessary to apply the chip protected because before every measurement, the glass surface has to be cleaned with a small paper slice and tweezers under the microscope. This was required as after every measurement and any new placing of the fibers, the fibers put a kind of gel on the glass. The protection of the bonding wires was also useful because the cleaning and the positioning process were safer. Overall, the chip worked very well after the preparations. However, after a power outage the chip was not able to read out the collected data from the chip anymore. During operating, the SiPM only delivered hit counts to the GUI. They behave as expected for the trigger and used overvoltage. But the frames were not displayed as usual. The chip itself seems to be working. Also, there were no optical hints on the chip or the bonding wires. The only reasonable explanation I found was that the chips' readout electronics were subjected to a high voltage for a short time. This could have happened because the PSU was connected to the board and the socket had no high-voltage protection. For the following analysis, a new chip used. This one is not protected by an additional cover glass. Working with this chip has been more difficult as it was necessary to act even more careful. The surface of the new chip has a coating which provides enough protection against plastic devices

[5]. In addition to this, the setup is also modified as to that the fibers are fixed in an additional way.

6. Scintillator - setup

In the following chapter, an improved setup will be presented. By using this, it is possible to detect atmospheric muons.

6.1 Setup

For the setup, the same location as in the chapters before was used, but in order to measure the full output of the scintillator bars it was necessary to put four fibers on the chip. I extended the setup by using an additional 5 m long WLS fiber, called „NULL“ fiber. This fiber collects photons emitted by LEDs and lamps close to the experiment. These photons appear on the chips' area where this fiber is placed. To have a defined position of the fibers on the chip, a special holding device was built by the workshop of the III. Physikalisches Institut A. It is made out of an 4 x 4 x 7 mm^3 aluminum block, shown in fig. 6.1. There are five 1.1 mm thick holes in it.

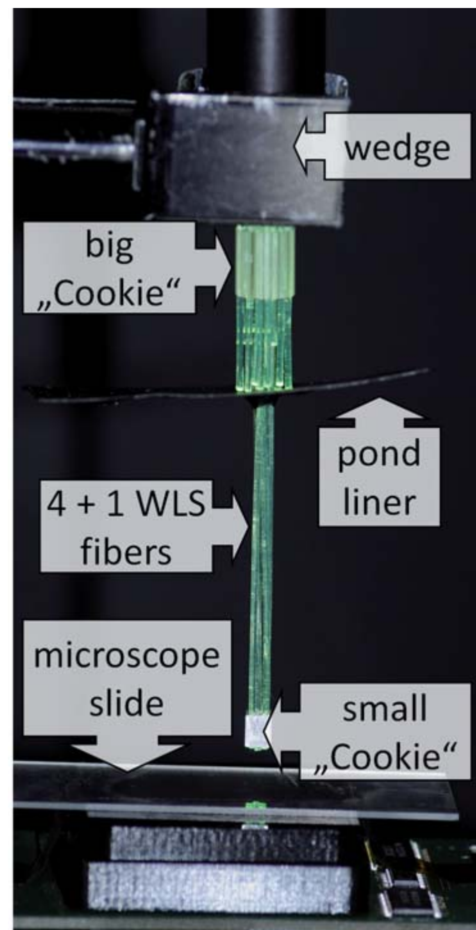

Figure 6.1: In this figure the preparation of the setup with the „Cookie“ is shown without the tweezers.

The preparation of this setup is more elaborated than the one of the others before: On one hand, the chip is now an unprotected one and on the other hand, the endings of all fibers have to be at the same height. To be sure about the height, a clean microscope slide is used as shown in figure 6.1. All fiber endings go through the metal tube in the wedge and through the big „Cookie“. The „NULL“ fiber is placed on the back side of the big „Cookie“. Only the fibers which are placed on the chip go through the small black pond liner. This piece of plastic

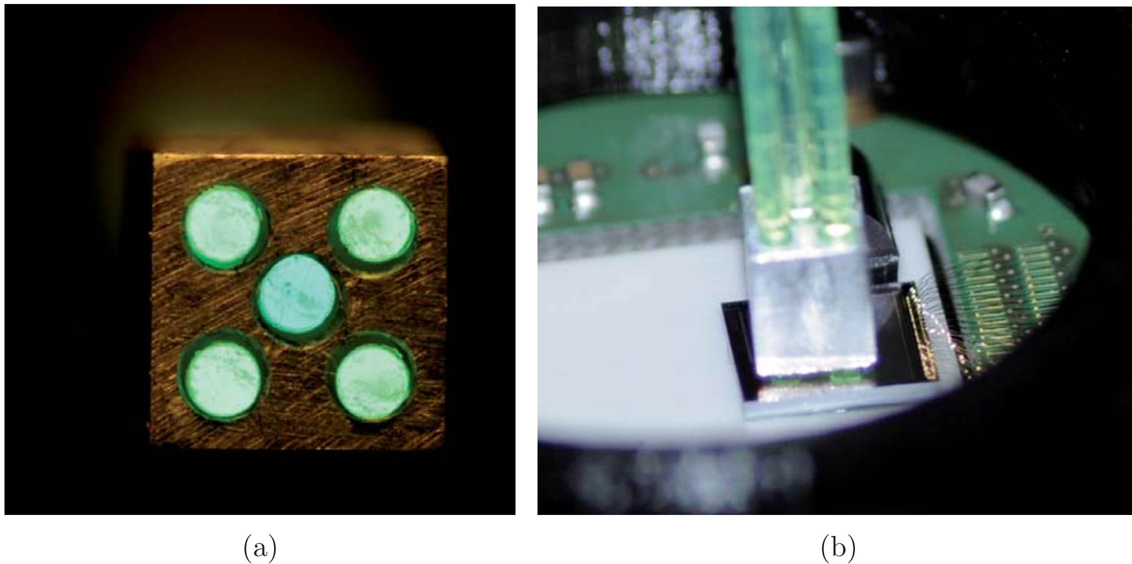

(a) (b)

Figure 6.2: a) The small „Cookie“ viewed from underneath. The WLS fiber in the middle appears to be brighter because this is the „NULL“ fiber. b) „Cookie“ placed on top of the chip's surface. The bare bonding wires are close to the „Cookie“. Only the endings of the fibers touches the surface.

shields the other photons emitted by the other fibers from the chip. Under the small „Cookie“, there is a microscope slide for positioning the endings at the same height. The additional fiber is placed in the middle hole of the „Cookie“.

After this has been done, the lid is opened and the HDROB is pulled up by a Z-table which is height adjustable. The final setup of the „Cookie“ is shown in fig. 6.2b. To make sure that the „Cookie“ does not touch the fibers, another „Cookie“ is placed ahead and held by X-tweezers. The tweezers are located in a vise to be stable in place. The scintillator bars are 165 cm long, 1 cm thick and 5 cm wide. This provides a horizontal detection area of 1650 cm^2. The scintillator bars are shown together with the WLS fibers in figure 6.3.

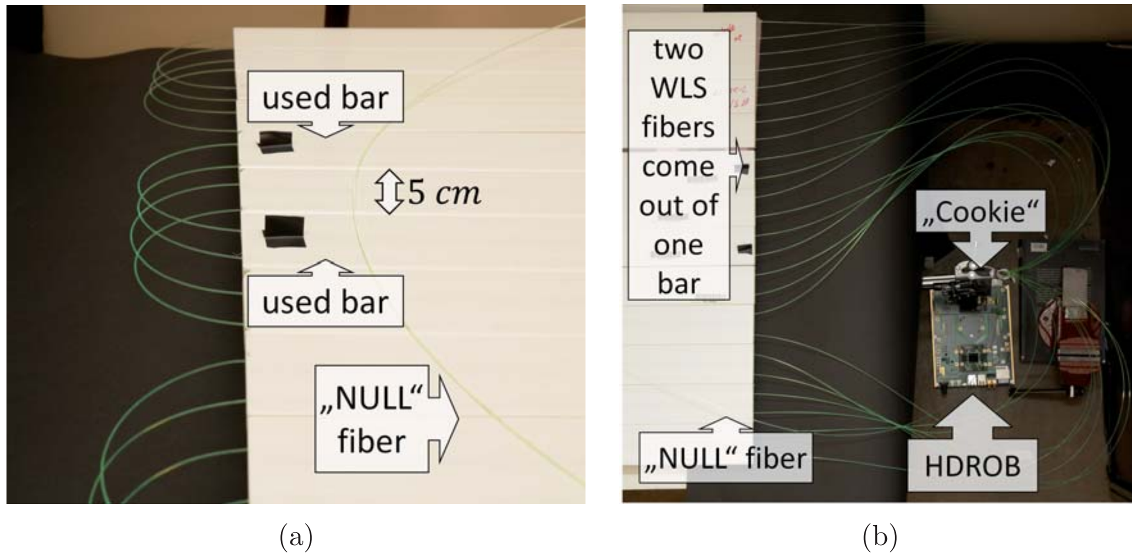

(a) (b)

Figure 6.3: Here, the endings of the scintillator bars are shown. Each bar holds two WLS fibers which go trough two different bars. The bars marked black are used for the measurements.

6.2 Measurement

For the measurements, the readout software was modified. While collecting data from the chip, the GUI saves the hit counts of every collected frame in an ASCII file. Additional to this, the software saves frames with more than 17 fired cells in another ASCII file. The advantages of these modifications are the possibility of viewing single frames and the frames being saved after a potential collaps of the GUI. The SiPM operates with an overvoltage of 3 V and the „mult $\geq$ 4“ trigger is used. Furthermore, no pixel was killed and the whole room was darkened to minimise the probability of stray light. The chip produces around 610, 000 fps. Only roughly 450 fps can be analysed by the read-out software. In other words, less than every thousandth frame could be saved. Unfortunately, it is not clear how the frames are selected. While taking different measurements, the values of hit count and readout speed were saved. The analysis of these values shows that the proportionals between these two are stable.

In figure 6.4, four single events are displayed. Events a) to c) were taken in a measurement with the five fibers on the chip. The photons were detected beneath the fibers, but not under the „NULL“ fiber in the middle of the setup. As a consequence, by high probability the photons come out of the scintillator bars by high probability. The events displayed in a) and b) have the highest measured hit counts. In c), an event is displayed where only some photons had come out of the fibers produced by the scintillator bars. The picture of the dark event in d) is one of a few with the highest hit count. For this measurement, the cover lid was closed to estimate the dark noise of the setup with the same conditions as in the measurement with the fibers on the chip.

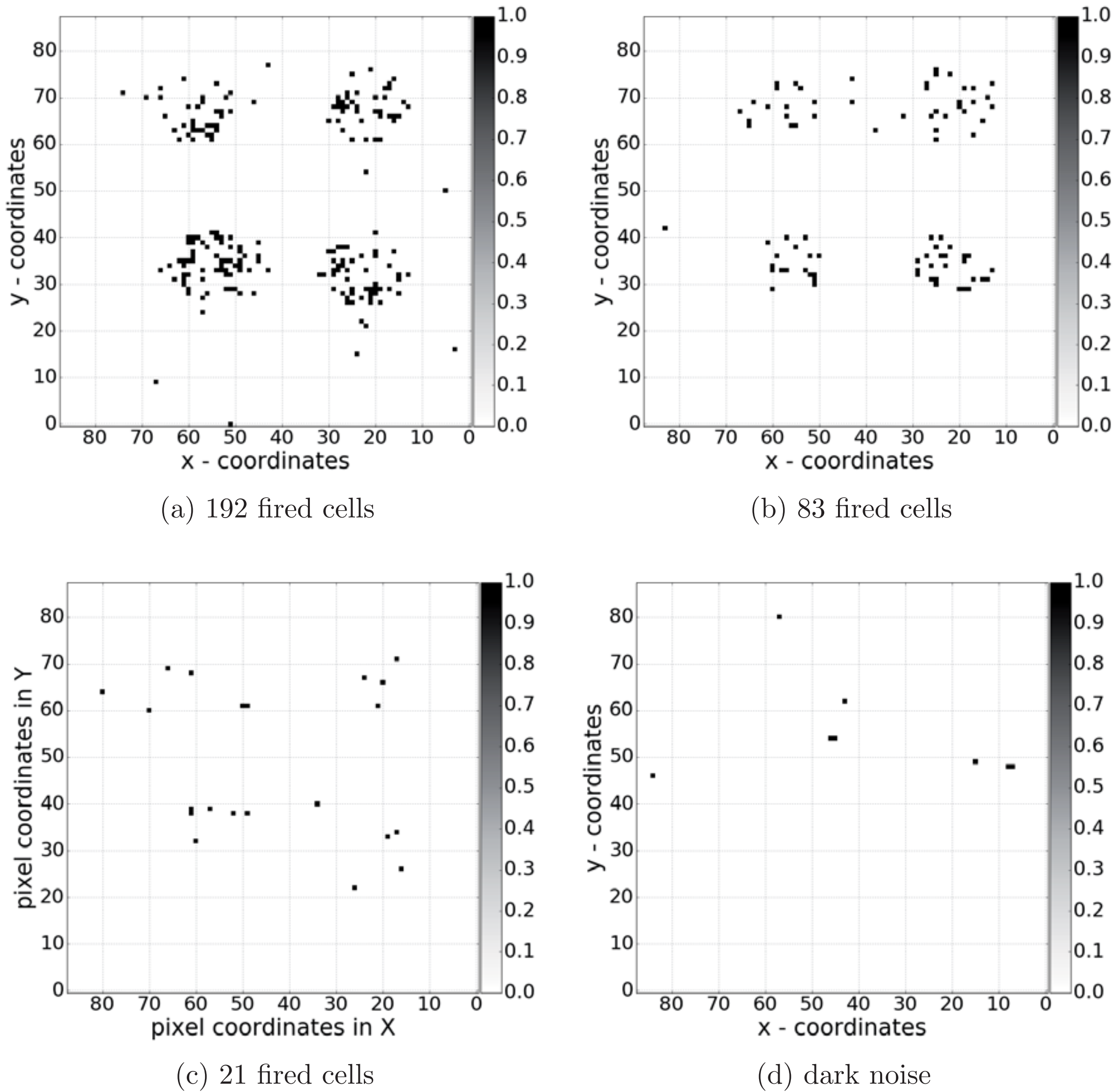

(a) 192 fired cells

(b) 83 fired cells

(c) 21 fired cells

(d) dark noise

Figure 6.4: Above, four single events with different counts are displayed. In a), b) and c), events with connected fibers are displayed. The most fired cells are beneath a WLS fiber. In d), an event of a dark measurement is shown.

6.3 Analysis

Two measurements were made for this analysis. The first is a dark measurement and is shown in figure 6.5. For this graph, the numbers of PE[1] of every event are summed up in a histogram. The counts are projected to the frame rate of the chip. For this, the entries are normed over the time of the measurement and projected to the rate of the chip.

Since the „mult $\geq$ 4“ trigger has been used, the expected maximum is at channel four which means that the most events collected had four fired cells. The histogram

[1]Photon Equivalent is a term when talking about analog SiPMs. Here it is used to describe the number of fired cells.

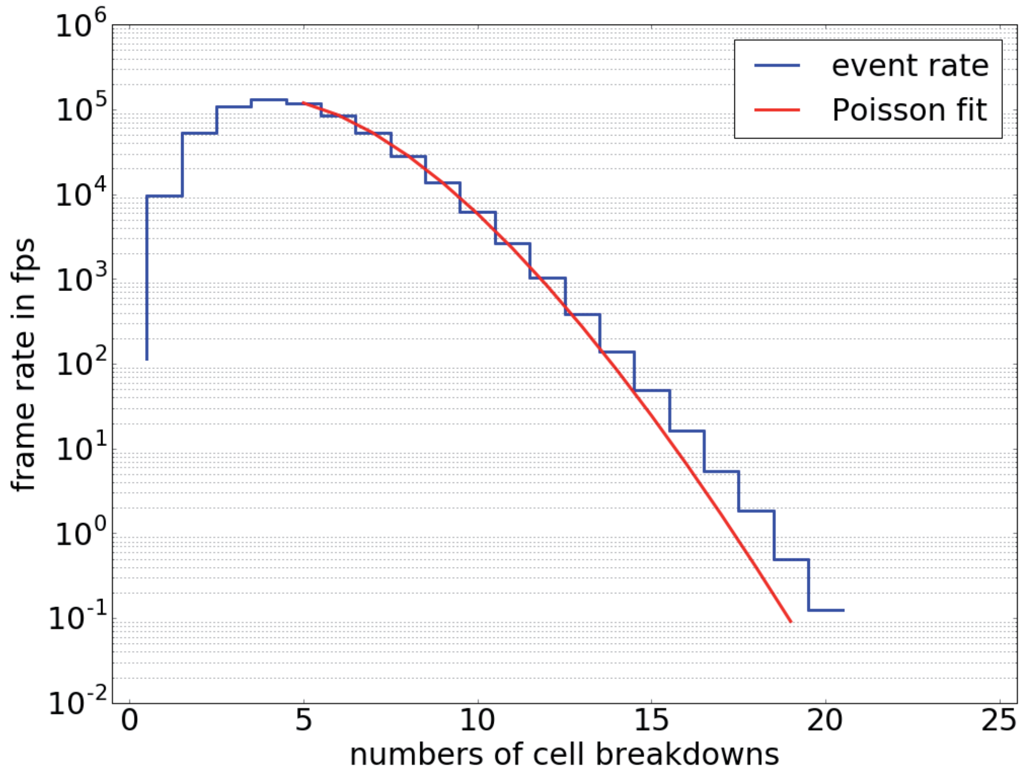

Figure 6.5: Here the results produced by the dark measurements are shown. The Poisson fit describes the decrease of the noise rate with an increasing number of cell breakdowns.

decreases with a Poission behavior and increasing number of PE. This is plausible since the frames are random events, occurring in a stable rate independent of each other. The highest PE of a dark event is 20. This event occurs during the dark measurement which took the same time as during the measurement with the fibers.

The second measurement was made with the small „Cookie“ on top of the chip with the same parameters as used in the dark one. The result is displayed in figure 6.6. As before, the noise rate decreases in a Poisson way. But after channel 20, the rate decreases slower. By summing up events with a higher PE than 20, the histogram shown in figure 6.7 is obtained. Most photons come out of the fibers and are neither raw noise signals nor background light of the room.

The chip's reading out speed is limited by 450 Hz. To be able to compare the results of the different measurement, there is a factor estimated by:

$$\Phi_{\text{scale}} = \frac{f_{\text{trigger rate}}}{f_{\text{readout rate}}} \tag{6.1}$$

$f_{\text{readout rate}} = (450 \pm 1.5)\,\text{Hz}$ is the actual readout rate with which the events are collected and saved. The frequency of the triggering is defined by the mean of 200 hit counts collected during the measurements to $f_{\text{trigger rate}} = (610,000 \pm 300)\,\text{Hz}$. With the factor $\Phi_{\text{scale}} = 1,350 \pm 1$ it is now possible to adjust the measured rates to

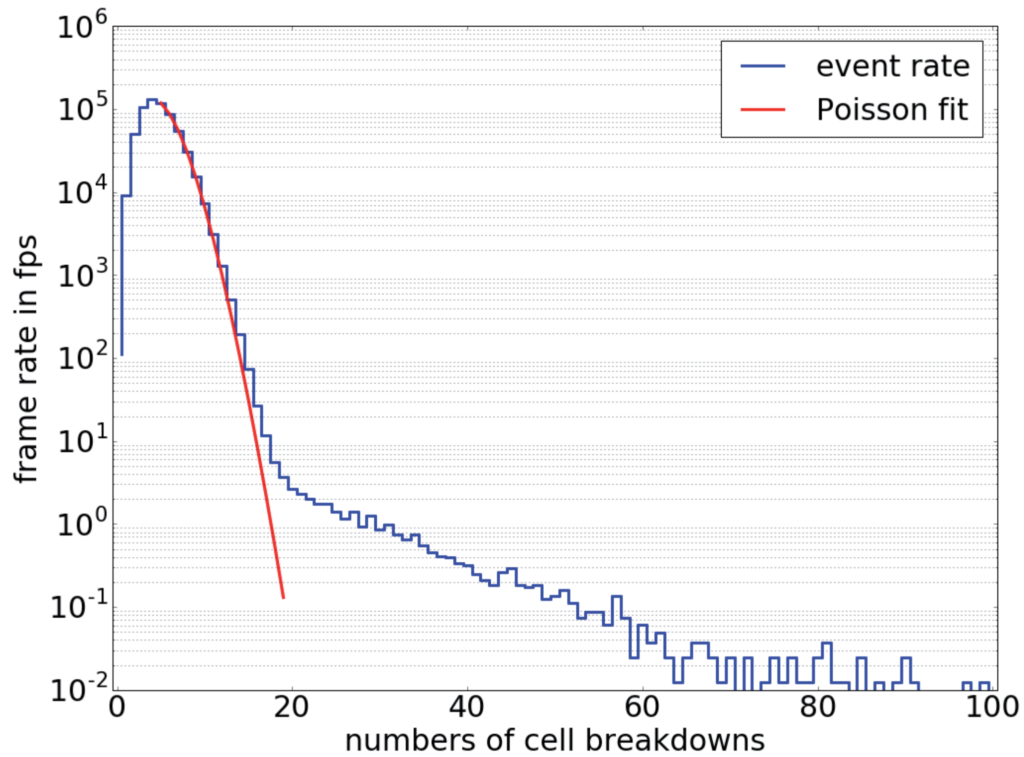

Figure 6.6: Above, the result of the measurement with fibers on top of the chip is shown. As in the measurement before the noise part decreases with a Poission behavior with an increasing number of PE.

the real triggered rates. The result of these scaling is shown in fig. 6.5 and 6.6. The integral below the shown event rate is in both cases the trigger rate of the chip.

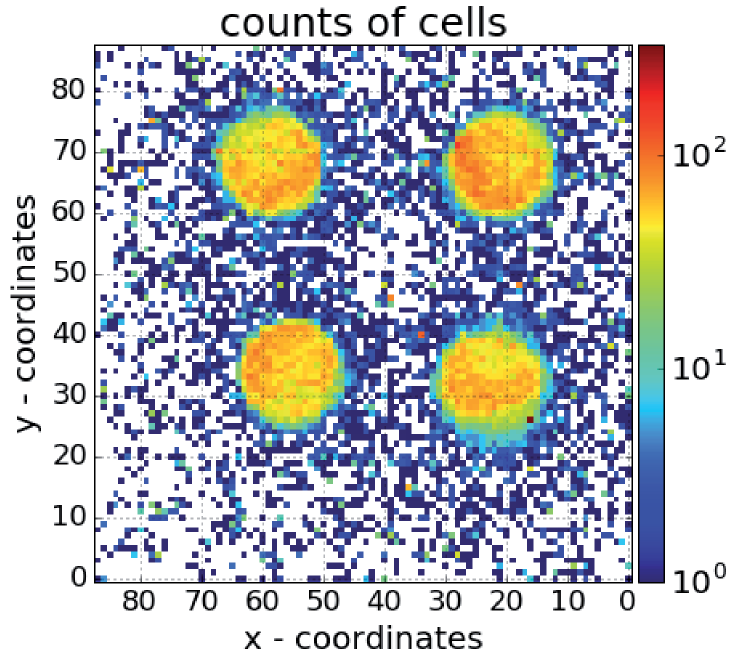

Figure 6.7: These are 1910 events summed up with a PE greater than 20. Only under the four fiber endings, which are going through the scintillator bars, photons are detected. The area under the „NULL“ fiber is empty, which implicates that the room was dark during the measurements.

Added together, the rate of the signals is (26.61 ± 0.03) fps. In other words this is a limit at which the setup measures a signal which occurs with more than 20 PE. This signal must come out of the scintillator bars. To compare the rate with predictions, it is converted to (0.96 ± 0.01) events $\cdot \mathrm{cm}^{-2} \cdot \mathrm{min}^{-1}$. With the scintillator material, it is possible to detect particles. As the setup is located in the first floor of a building with five floors, the setup is shielded by four floors in the vertical. Only muons made by air showers have the highest probability to reach the scintillator bars through this shielding. If a muon goes through the bar, it creates about 100 photons at the end of the fibers. This is the result of similar measurements with the setup [14]. The literature suggests a value for an expected muon rate up to $1\,\mathrm{cm}^{-2} \cdot \mathrm{min}^{-1}$ [15, chapter 29]. The measurement is consistent with this value.

7. Summary and Outlook

In this thesis, a newly developed photo-sensitive device was tested. The results are promising. The tested digital SiPM worked very well during the measurements. The chip is suitable for various applications. It can be used to test optical components, to test whole optical setups or to detect photons produced by scintillator bars. In the case of this thesis, the expected atmospheric muon rate was measured at $(0.96 \pm 0.01)\,\mathrm{cm}^{-2} \cdot \mathrm{min}^{-1}$ which is consistent with the typical value found in literature.

The digital SiPM has even more features which can be used in different contexts. The next firmware will increase the readout speed enormously. It will also be possible to measure with frames in a frequency around 100 MHz.

References

[1] Niggemann, T. et al., Pierre Auger Collaboration internal note (2012).

[2] Renker, D. and Lorenz, E., IOP science (2009).

[3] Fischer, P., Novel Fast and Position Sensitive Photo Detectors based on SiPMs and SPADs, GK Seminar at Department of Physics at RWTH Aachen, 2016.

[4] Frach, T. et al., The Digital Silicon Photomultiplier - Principle of Operation and Intrinsic Detector Performance, in *Nuclear Science Symposium Conference Record*, Nuclear Science Symposium, IEEE, 2009.

[5] Fischer, P., personal communication after presentation in Aachen on the 13th December 2016.

[6] Sacco, I., *Development of highly integrated PET/MR detector modules*, PhD thesis, Combined Faculties for the Natural Sciences and for Mathematics of the Ruperto-Carola University of Heidelberg, 2016, chapter 7.3 a digital photon counter.

[7] Thil, C., *Digital SiPM ASIC and Readout System Quick Start Guide*, 2015.

[8] *Product Information Sheet Borofloat 33*, 2014, adress =http://www.vdg-ev.org/technik/kataloge/schott/.

[9] EPOXY Technology, *Product Information Sheet EPO-TEK 310M-2*, 2012, adress http://www.epotek.com/site/component/products/.

[10] Fischer, A. C. et al., IOP science (2013).

[11] panacol adhesives & more, *Technisches Datenblatt Vitralit 1671*, 2014, adress =http://www.panacol.de/produkte/datenblaetter/.

[12] Bretz, T. et al., FAMOUS – A fluorescence telescope using SiPMs, The 34th International Cosmic Ray Conference, 2015.

[13] Peters, C., personal communication.

[14] Kemp, J., personal communication.

[15] Patrignani, C. et al., Chin. Phys. **C40** (2016) 100001.

Acknowledgements

In erster Linie möchte ich mich bei meinem betreuenden Jun. Prof. Dr. Thomas Bretz bedanken, der mir die Möglichkeit gegeben hat, diese Bachlorarbeit zu verfassen. Weiterhin gilt mein Dank Herrn Prof. Dr. Thomas Hebbeker, welcher als Leiter des III. Physikalischen Instituts A mir die Arbeit hier ermöglichte und diese als Zweitkorrektor bewerte.

Außerdem möchte ich Herrn Prof. Dr. Peter Fischer von der Universität Heidelberg dafür danken, dass er keine Kosten und Mühen gescheut hat, um mich nach einem unvorhergesehenen Rückschlag, mit einem neuen Chip auszustatten, um meine Forschungsarbeit fortsetzen zu können.

Besonderen Dank gilt meinen beiden Büronachbarn, Johannes Schumacher und Lukas Middendorf, welche jederzeit bereit waren mich in jedweder Hinsicht zu unterstützen. Dabei hat Johannes sehr viele Stunden in die Betreuung dieser Arbeit gesteckt, wofür ich ihm sehr dankbar bin. Des Weiteren möchte ich mich auch bei den weiten 'Hallenbewohnern' bedanken, welche mich tatkräftig auf ihren jeweiligen Gebieten unterstützt haben: Herrn Philipps als Leiter der Werkstatt, Julian Kemp als Fachmann für optische Bauelemente, Dr. Karl als gute Seele der Halle, sowie Christine Peters, welche stets bei offenen Fragen zur Stelle war, möchte ich speziell danken.

Ich möchte mich bei allen Mitarbeitern des III. Physikalischen Instituts bedanken, da alle zusammmen eine sehr angenehme Atmosphäre zum Forschen gebildet haben.

Abschließend bedanke ich mich bei meiner Familie und meinen Freunden, welche mir stets zur Seite standen.

Erklärung

Hiermit versichere ich, dass ich diese Arbeit einschließlich beigefügter Zeichnungen, Darstellungen und Tabellen selbstständig angefertigt und keine anderen als die angegebenen Hilfsmittel und Quellen verwendet habe. Alle Stellen, die dem Wortlaut oder dem Sinn nach anderen Werken entnommen sind, habe ich in jedem einzelnen Fall unter genauer Angabe der Quelle deutlich als Entlehnung kenntlich gemacht.

Aachen, den 30. Januar 2017

Robert Joppe